2012 15th International IEEE Conference on Intelligent Transportation Systems
Anchorage, Alaska, USA, September 16-19, 2012

Evolutionary Approach to Calibration of Cellular Automaton Based Traffic Simulation Models

Pavol Korcek, Lukas Sekanina and Otto Fucik

Abstract— **Microscopic traffic simulation models have become very popular in the evaluation of transportation engineering and planning practices in the past few decades. To achieve high fidelity and credibility of simulations, a model calibration and validation must be performed prior to deployment of the simulator. In this paper, we proposed an effective calibration method of the microscopic traffic simulation model. The model is based on the cellular automaton, which allows fast large-scale real-time simulation. For its calibration, we utilized a genetic algorithm which is able to optimize different parameters much better that a human expert. Furthermore, it is possible to readjust the model to given field data coming from standard surveillance technologies such as loop detectors in our case. We have shown that the precision of simulations can be increased by 20 % with respect to a manually tuned model.**

I. INTRODUCTION

Microscopic traffic simulation models distinguish and trace every single vehicle and driver on the road. These models typically employ the characteristics such as individual vehicle speeds, accelerations, time and distance headways to the preceding vehicle or some rudimentary human characteristics that describe driving behavior [1], [2]. This allows us to simulate the traffic very precisely. Today, the microscopic traffic simulation software is widely accepted and applied in all branches of transportation engineering as an efficient and cost effective analysis tool. On the other side, a lot of modeled entities extremely increase the simulation time.

A. Model performance

In case when the simulation is used as a part of a complex ITS (e.g. for online traffic states prediction), the simulation time becomes extremely critical. To be able to simulate large traffic at the microscopic level of detail, different acceleration techniques have already been developed. Some of them utilized special hardware [3], other ones employed multicore architectures or even high performance graphic cards [4] that are becoming parts of nowadays commodity hardware too. The simulation time significantly depends on the traffic model representation (e.g. form of the model). It seems that a reasonable representation is used when the traffic is simulated with cellular automaton (CA) based models. Recently, CA have become popular in the area of microscopic traffic simulations because of their simplicity and suitability for acceleration. For example, in paper [5], an online CA based simulation model of city of Duisburg was introduced. The authors showed that for the most frequently occurring densities the road network of Duisburg can be simulated around 100 times faster than real time. It is necessary to mention that their road network is modeled using only 22 000 cells and their simulator is not suitable for more cells. An example of explicitly implemented parallelism in a simulation model was presented in [6]. The authors have used a CA model to implement a traffic simulator for city of Geneva and they reported a super linear speed-up for 15 000 vehicles. However, their simulations are not expected to match the exact traffic situation of Geneva, as they mentioned. CELLSIM is another good example of a recent CA based microscopic simulator [7]. Computational performance of this model, as for other microscopic models, is dependent on the number of vehicles in the system. It was shown, that CELSIM is able to simulate around 2300 vehicles in shorter than real time. As computational power is constantly increasing, we can assume that this number of vehicles will increase too.

In our previous work, we also utilized such techniques to speed-up our large-scale CA based model with special libraries for explicitly programmed parallel model for multicore processors [8] or for modern graphic cards [9], which allowed us to simulate huge networks (e.g. 935 000 km with 50% crowdedness) multiple in real-time.

B. Model quality

However, not only the performance is crucial in microscopic traffic simulation models. A very important stage of development of any traffic model is its comparison with reality, namely calibration and validation. In [10], authors proposed an effective three-step process for the microscopic traffic model calibration. Another paper [11] gives some basic guidelines for calibration of microscopic simulation models in form of framework and applications. The developers usually calibrate and validate the model on their own using some data sets that they have access to and publish the results obtained. For example, in paper [12] authors tried to perform a simple calibration of ten microscopic traffic simulation models in a way that the models were calibrated and compared to each other with the GPS based field data from year 2004 in Japan. But it should be noted, that in almost all previous calibration approaches, some real data are desired in a form, which is not generally available. It was shown that it is important to find a few basic parameters for the model calibration [13]. Namely a driver sensitivity

This work was partially suported by the Czech Science Foundation under projects P103/10/1517 and GD102/09/H042, by the IT4Innovations Centre of Excellence project CZ.1.05/1.1.00/02.0070, by the research program MSM 0021630528, FIT BUT grant FIT-S-12-1 and CAMEA spol. s r. o.

Pavol Korcek, Lukas Sekanina and Otto Fucik are with Brno University of Technology, Faculty of Information Technology, IT4Innovations Centre of Excellence, 612 66 Brno, Czech Republic {ikorcek, sekanina, fucik}@fit.vutbr.cz.

978-1-4673-3063-3/12/$31.00 ©2012 IEEE

(e.g. reaction time), a jam density headway and free-speed (maximum speed when vehicle is not constrained) have to be determined. It was also stated that this process is neither a straight-forward nor an easy task. For example, while the free-speed is relatively easy to estimate in the field and generally lies between the speed limit and the design speed of the roadway, the jam density headway is more difficult to calibrate but typically ranges between 110 to 150 vehicles/km/lane. The driver sensitivity factor is extremely difficult to calibrate because it can not be measured using standard surveillance technologies (e.g. detection loops that work on magnetic-induction principle).

C. Goals of the paper

In this work we propose to utilize our CA based microscopic traffic simulation model, which was shown not only to be extremely fast to achieve multiple in real-time simulations, but also updated to eliminate unwanted properties of ordinary CA based models. The quality of this updated model has been previously evaluated by comparison with fundamental diagrams and discussed [8]. Secondly, we will try to calibrate parameters of this model to various field data that can be obtained from standard surveillance technologies. We will show, that it is possible to achieve a better precision of simulation for a given road segment. Moreover, except ordinary traffic parameters, we will also optimize some CA model parameters as well as calibrate some parameters which, as stated for example in [13], are extremely difficult to calibrate with other common techniques. The optimization/calibration will be performed by genetic algorithm (GA).

The rest of the paper is organized as follows. Section II introduces a stream model calibration technique that allows us to fairly compare real data with the calibrated simulation model. Then, in Section III, cellular automaton based microscopic traffic simulation model is presented with all its updates and parameters utilized in the process optimization. Section IV describes the process of optimization of the model with selected GA. Results of experimental evaluations for each field data set are then presented in Section V. Finally, conclusions and suggestions for future work are given in the last Section VI.

II. STREAM MODEL CALIBRATION

Gazis et al. [14] were the first ones who formulated a relation between microscopic and macroscopic traffic models. In their theory, the flow rate can be expressed as the inverse of the average vehicle time headway. Similarly, the traffic stream density can be approximated for the inverse of the average vehicle spacing for all vehicles within a section of the roadway.

Road traffic is always in a specific state that can be characterized by three macroscopic parameters: flow (q), vehicle space-mean speeds (u) and density (k) shown in Eq. 1:

$$q = k \times u. \tag{1}$$

By combining all the possible traffic states (steady or non-steady) in an equilibrium function, one can derive three fundamental traffic diagrams [15]. A diagram shows the relation between two of the three variables (speed-density, speed-flow, flow-density). The third variable can always be recovered using Eq. 1.

It was shown [16], that estimation of the traffic stream parameters requires the calibration of a traffic stream model to field data. This effort entails making some decisions, such as defining the functional form to be calibrated, identifying dependent and independent variables, defining the optimum set of parameters, and finally developing an optimization technique to compute the set of parameter values. Unfortunately, in the traffic flow theory it is not always clear which variable should be set to be independent or dependent. In paper [13] and later in [17], authors developed a calibration approach that minimizes the orthogonal error about the fundamental diagram to estimate the expected value of the traffic stream parameters. The model, which is also used to preprocess our data, is briefly described here, however a more detailed description can be found in [17]. Also, this approach is unique because it does not require the identification of dependent or independent variables since it applies a neutral regression (i.e. minimizes the orthogonal error as shown in Eq. 2).

$$E = \sum_i \left\{ \left(\frac{u_i - \widehat{u_i}}{\widetilde{u}}\right)^2 + \left(\frac{q_i - \widehat{q_i}}{\widetilde{q}}\right)^2 + \left(\frac{k_i - \widehat{k_i}}{\widetilde{k}}\right)^2 \right\} \tag{2}$$

where $\forall i$:

$$\widehat{k_i} = \frac{1}{c_1 + \frac{c_2}{u_f - \widehat{u_i}} + c_3 \widehat{u_i}}$$

$$\widehat{q_i} = \widehat{k_i} \times \widehat{u_i}$$

$$\widehat{q_i}, \widehat{k_i}, \widehat{u_i} \geq 0$$

$$\widehat{u_i} < u_f$$

and

$$0.5 u_f \leq u_c \leq u_f$$

$$q_c \leq \frac{k_j u_f u_c}{2u_f - u_c}$$

$$c_1 = \frac{u_f}{k_j u_c^2} (2u_c - u_f)$$

$$c_2 = \frac{u_f}{k_j u_c^2} (u_f - u_c)^2$$

$$c_3 = \frac{1}{q_c} - \frac{u_f}{k_j u_c^2}$$

$$u_f^{min} \leq u_f \leq u_f^{max}; u_c^{min} \leq u_c \leq u_c^{max}$$

$$q_c^{min} \leq q_c \leq q_c^{max}; k_j^{min} \leq k_j \leq k_j^{max}$$

where u_i, k_i, and q_i are the field observed space-mean speed, density, and flow measurements, respectively. The speed, density, and flow variables with hats are estimated speeds, densities, and flows while the tilde variables are the maximum field observed speed, density, and flow measurements.

c_1, c_2, and c_3 are then selected model constants. The objective function ensures that the formulation minimizes the normalized orthogonal error between three-dimensional field observations and the functional relationship – in this case the *Van Aerde* functional form is utilized. The error terms are normalized in order to ensure that the function is not biased towards reducing the error in one of three variables at the expense of the other two variables. This data normalization ensures that the parameters in each of the three axes range from 0.0 to 1.0 and thus a minimization of the orthogonal error provides fitting equivalent across all three axes. The initial constraint, which is non-linear, ensures that the Van Aerde functional form is maintained, while the second constraint is added to constrain the third dimension, namely the flow rate. The third and fourth set of constraints guarantee that the results of the minimization formulation are feasible. The fifth and sixth set of constraints ensures that the four parameters that are selected do not result in any inflection points in the speed-density relationship (e.g. it ensures that the density at any point is less than or equal to the jam density). Next set of equations provides estimates for three model c-constants [18] based on the roadways mean free-flow speed (u_f), speed at capacity (u_c), capacity flow (q_c), and jam density (k_j). The final set of constraints provides a valid search window for four traffic stream parameters that are being optimized (u_f, u_c, q_c, and k_j). All details can be found in paper [16].

The primary goal for using this stream model calibration to the field data sets is to fairly compare the real data with results obtained from the calibrated simulation model. So it is possible to get all three fundamental traffic diagrams, which is very important, because a good fit in one domain (e.g. speed-flow) does not necessarily imply a good fit in another domain (e.g. speed-density) [16].

III. CA BASED TRAFFIC SIMULATION MODEL

The first highly suitable CA model of single-lane freeway traffic was introduced by Nagel and Schreckenberg in 1992 [19]. Because of simplicity of this model, it was possible to perform millions of updates in a second [20]. Hence, the model can be used for simulating a high volume of traffic over very large networks. Due to some critics of unrealistic behavior (such as [21]), simple CA based models are often extended. On the other hand, these models were shown to be able to capture all basic phenomena that occur in traffic flows [22], not only in the field of vehicular traffic flow modeling, but also in other fields such as pedestrian behavior, escape and panic dynamics, etc.

Nagels and Schreckenbergs traffic model was initially defined on a one-dimensional array with open or periodic boundary conditions and with every single cell representing a road segment [19]. A local transition function (a rule) defines the new state of a cell on the basis of its current state and the state of neighboring cells. Globally viewed, it describes the movements of vehicles from one cell to another cell in a discrete way. In space domain, each cell represents only a defined length of road segment, so space is coarse-grained. This coarse graininess is fundamentally different from the usual microscopic models, which adopt a semi-continuous space. The length of 7.5 m was chosen in the original model because each car occupies about this amount of space in a complete jam [19]. In other words, this is the average vehicle length on the road, including a constant gap in front of and/or behind each car. In order to model other kinds of vehicles in CA based models, it is better to use different cell lengths, or even more precisely, use more smaller cells for representing a single vehicle – especially for bigger types of vehicles (e.g. [23]).

Each CA simulation step represents an amount of time in reality. In the CA model this value is crucial because together with the cell length it gives us the granularity of minimal vehicle speed jumps. This value also represents a minimal time for any responds, e.g. it is also the driver reaction time. Based on suggestions given in [24] and field data measurements [23], it is reasonable to consider one such simulation step as 0.6 – 1.5 s.

Normally, urban traffic road networks are very complex. It was shown that arbitrary kinds of road and intersections can be reduced to only a few basic elements. For constructing more complicated networks, we shall simply connect more various kinds of cells to the desired topology. In this way it is possible to build more traffic lanes, roundabounds or very complex topologies for whole cities [6], [5].

A. Local transition function

Properties of a single lane traffic are modeled on the basis of integer-valued probabilistic cellular automaton rules. The local transition function can be formalized as follows: each vehicle (i) in a cell has an integer velocity $v_v(i)$ with values between zero and $v_{max}(i)$. We let $gap(i)$ denote the cell gap in front of the vehicle i – i.e. a leader to the follower distance. For an arbitrary configuration, one update of the simulation system consists of four consecutive steps, which are performed in parallel for all vehicles. The original procedure consists of (1) acceleration (every vehicle tends to accelerate), (2) slowing down (i.e. collision avoidance), (3) randomization with a given probability and finally (4) vehicle motion, where each vehicle is advanced based on a new computed speed $v_v(i)$. It is important to note, that this simple CA based traffic model shows nontrivial and realistic behavior. The randomization step is essential in simulating traffic flows since the model dynamics is completely deterministic, and without this randomness, every initial configuration of vehicles and corresponding velocities reaches a stationary pattern which is shifted backwards. This simple model is also capable of reproducing characteristic properties of real traffic, such as certain aspects of flow-density relation, spatio-temporal evolution of jams, stop-and-go waves, etc. [25].

B. Updated local transition function

In our previous work [8], we updated the original function briefly described in previous section to a new form, where some brand new parameters can be found. The traffic simulation model is extended to eliminate unwanted properties of ordinary CA based models, such as stopping from maximum velocity to zero in one time step [8]. This is possible due to storing the previous (or the leading) vehicle velocity $v_{prev}(i+1)$. When there is such vehicle, the following vehicle (i) is able to determine its positive or negative acceleration with $acc(i+1)$. According to Alg. 1, it is firstly determined, if investigated vehicle could accelerate (i.e. vehicle velocity $v_v(i)$ is not greater than maximal vehicles speed p_4 or given vehicle velocity limit $v_{max}(i)$). If so, its speed-up is accomplished with probability p_7, so not all vehicles tend to always accelerate as in the original model [19]. Then, if there is a plenty of room for vehicle to get in (i.e. $gap(i)+acc(i+1) > v_v(i)$) or there is no previous vehicle in the same lane, collision avoidance mechanism is not performed. Similarly to the original CA local transition function, only deceleration based on probabilities could be applied in this situation. In case of small vehicle velocities ($v_v(i) < p_6$), deceleration is performed with probability p_5, otherwise ($v_v(i) > p_6$) with probability p_8.

Algorithm 1 Updated local transition function.

```
if $v_v(i) < p_4$ and $v_v(i) < v_{max}(i)$ then
    $v_v(i) := v_v(i) + 1$ with probability $p_7$
end if
if $(gap(i) + acc(i+1)) > v_v(i)$ then
    if $v_v(i) < p_6$ then
        $v_v(i) := v_v(i) - 1$ with probability $p_5$
    else
        $v_v(i) := v_v(i) - 1$ with probability $p_8$
    end if
else
    if $acc(i+1) > 0$ then
        $v_v(i) := 1/p_9 \times (gap(i) + acc(i+1))$
    else
        $v_v(i) := 1/p_{10} \times (gap(i) + acc(i+1))$
    end if
end if
```

Ensure: Each vehicle at sites i is advanced $v_v(i)$ times and $v_{prev}(i) := v_v(i)$.

Collision avoidance occurs when there is no free room for vehicle i in the same lane to get in (i.e. $gap(i) + acc(i+1) <= v_v(i)$). Two situations may occur. If the leading vehicle tends to accelerate ($acc(i+1) > 0$), the actual vehicle velocity $v_v(i)$ is reduced to $1/p_9 \times (gap(i) + acc(i+1)$. Otherwise, ($acc(i+1) <= 0$), actual vehicle speed $v_v(i)$ is reduced to $1/p_{10} \times (gap(i) + acc(i+1)$. It can be seen that these two parameters are more driver-based parameters than model oriented. We will try to find out if these ones could be determined statistically for a given road segment. Finally, each vehicle is advanced $v_v(i)$ sites and vehicle velocity updates must be also performed.

IV. OPTIMIZATION OF THE CA BASED MODEL

In this work, genetic algorithm (GA) is used to find the most useful parameters of the CA model in order to maximize the precision of the traffic simulator. The main idea of GA is to evolve a population (set) of candidate solutions to find better ones [26]. Such candidate solution is encoded as a chromosome which is an abstract representation that can be modified with genetic operators (e.g. mutation and crossover, etc.).

A. Parameters encoding

In order to simplify GA, all simulation model parameters, which will be optimized, are encoded in binary form. In case of real numbers from a given interval (e.g. $[1, 0]$), the interval is divided into the N pieces of the same size. The value N depends on the number of bits used for encoding of the parameter.

Using a 6-bit value and the minimal length of the cell 0.125 m the maximal cell length is 8 m (64×0.125). The cell length is the first model parameter – p_1. One vehicle always occupies as many such cells as it fits into the 5.5 m (or nearer, but not smaller). For example, for the smallest cell length (0.125 m) it is exactly 44 cells. Bigger vehicles, such as trucks, occupy only two times bigger place (11 m). The second model parameter, p_2, is the simulation step or also the reaction time with the minimal value of 0.05 and maximum value of 3.2 seconds encoded again using 6 bits. The cell neighbor, p_3, is encoded using 12 bits (e.g. when the cell length is at minimum then the maximum neighbor is $0.125 \times 4096 = 512$ m). The next parameter is maximal vehicles speed p_4 (encoded on 11 bits, i.e. 2048 possible values for a chosen reaction time and cell lenght) giving, as in the original model, the number of cells per simulation step. The probability of slowing down is represented by p_5 (encoded on 8 bits) and slow speed boundary is encoded as p_6 ($1 - 512$ cells per simulation step on 9 bits). Then, the speed-up probability is denoted as p_7. The parameter p_8 is probability of vehicles slowing down in case of a vehicle speed greater than the slow speed p_6. Further model constants p_9 and p_{10} are coefficients of vehicle approximation in case of previous vehicle acceleration and previous vehicle slowing-down. Both parameters have minimal value of 1 and maximal value of 32 (encoded on 5 bits). All parameters with their respective minimal values, maximal values and step, are briefly summarized in Tab. I.

B. Chromosome

The proposed GA has an auto-evolution or also self-adaptation capability, which means that parameters of the algorithm (the probability of mutation p_m and crossover p_c) are also part of the chromosome. Hence the user is not forced to set them. The whole set of parameters is represented using one 92-bit number. It is important to note that each parameter of the chromosome is encoded using *Gray encoding* to ensure that the maximal Hamming distance between two successive values is only one. This setup does not allow big jumps between values in case of a single bit change. The

TABLE I: CA model parameters and values.

	Bits used [#]	Min. value	Max. value	Step
p_1	6	0.125	8.000	0.125
p_2	6	0.05	3.20	0.05
p_3	12	p_1	$2^{12} \times p_1$	p_1
p_4	11	p_1/p_2	$2^{11} \times p_1/p_2$	p_1/p_2
p_5	8	0.00392	1.00000	0.00392
p_6	9	p_1/p_2	$2^9 \times p_1/p_2$	p_1/p_2
p_7	8	0.00392	1.00000	0.00392
p_8	8	0.00392	1.00000	0.00392
p_9	5	1	32	1
p_{10}	5	1	32	1
p_m	10	0.00097	1.00000	0.00097
p_c	4	0.06667	1.00000	0.06667

first population ($X(0)$) consists of 60 such chromosomes ($|X(0)| = 60$) generated randomly.

C. Fitness function

All chromosomes from population X_i are separately evaluated using the same fitness function. Firstly, a candidate CA model is constructed using the parameters obtained from a candidate chromosome. Then simulation is performed for the given model. Because field data usually consists of various scenarios over different traffic speeds, densities and flows, it is possible to initialize the new model with *random data* inputs (e.g. random times of vehicle arrivals) to gather different flow/density/speed situations from calibrated model. Note, that this random data generation could be notably simplified, if the average incoming vehicle speed and also the average incoming times with their respective variability are enumerated from given field data set. Whole measurement procedure (from the simulation model) is performed in same way as measurements from the field, which will be described later on. Depending on the facility type, also various vehicle types are generated where possible. Whole simulation is executed until the same number of samples (flow vs. speed and flow vs. density) as the number of field data samples is reached (see Tab. II). After that, the fitness function $F(x)$ is calculated as a sum of error function $E(x)$ (shown in Eq. 2) and the penalty function $P(x)$, where x represents a candidate solution. Due to noticeable slower simulation runtime for solutions where the cell length is very small, the fitness function must be adjusted with the penalization function $P(x)$ as showh in Eq. 3.

$$P(x) = 10/cel\_length(x) \tag{3}$$

This penalization ensures that the solutions with smaller cell lengths will not be preferred. Moreover, this penalization is multiplied three times (the error function is calculated for three different variables separately) and also multiplied by the number of samples (to add a constant error to every sample) as shown in Eq. 4.

$$F(x) = E(x) + (3 \times number\_of\_samples(x) \times P(x)) \tag{4}$$

Finally, GA tries to minimize the fitness function $F(x)$, so better solutions are always with lower fitness value.

D. Creating a new population

1) Selection: After evaluation of all chromosomes from the population $X(i)$ is complete, some of them are selected for next operations using a tournament selection with base 2 giving a new population $X_S(i)$, where $|X_S(i)| = 30$.

2) Crossover: Two-point crossover is applied between two randomly selected individuals giving a new set $X_C(i)$ (where $X_C(i) \subset X_S(i)$ and $|X_C(i)| = 30$). The first point of crossover operation is between the p_3 and p_4 parameter and the second one right after p_{10} parameter, to allow alternation of the model and the GA parameters individually. This operator is applied with the average probability calculated from two chosen chromosomes (p_c).

3) Mutation: On all chromosomes from $X_C(i)$ a mutation operator (i.e. changing bit $0 \rightarrow 1$ or $1 \rightarrow 0$) is applied with the probability (p_m) taken from evaluated individual, which gives a brand new population $X_M(i)$ of the same size.

4) Population recovery: Finally, a new population of 60 individuals $X(i+1)$ is selected from the previous population $X(i)$ and the $X_M(i)$ population. This ensures that the best solution will always survive (i.e. elitism is present) [26].

Described GA procedure is repeated until 125 000 generations are exhausted as shown in Alg. 2.

Algorithm 2 Genetic algorithm procedure.

```
$i = 0$
Generate population $X(i)$ randomly, $|X(i)| = 60$
Evaluate all candidates from $X(i)$ with $F(x)$
repeat
    1. Create $X_S(i)$ using tournament selection from $X(i)$
    2. Create $X_C(i)$ using crossover operator on $X_S(i)$
    3. Create $X_M(i)$ using mutation operator on $X_C(i)$
    4. Evaluate all candidates from $X_M(i)$ with $F(x)$
    5. Create $X(i+1)$ by selecting 60 best individuals from $X_M(i) \cup X(i)$
    6. $i := i + 1$
until ($i <= 125000$)
```

V. Experimental Results

A. Field data

In order to evaluate the proposed method, field data from different facility types have been utilized. These macroscopic data sets consist of data captured by our industrial partners in year 2010.

The first data set (a) is a bit crocked road segment between two bigger villages in the Slovak Republic with a maximum allowed speed of 50 km/h. The particular segment is on the way to the country seat, so the road is utilized mostly by drivers going to work and back on ordinary business days, but traffic is not strictly homogenous here. This road segment is also a part of the route between two biggest cities in the region and statistically given 5% of traffic comes from bigger vehicles (e.g. busses, trucks, etc.).

The second data set (b) comes from two climb-lanes on the freeway road segment between two biggest cities in

TABLE II: Number of field data samples for each data set.

Data set	Usable samples [#]	Empty samples [%]
(a)	31157	11.08
(b)	32268	7.91
(c)	29396	16.11

TABLE III: Parameters and per point errors for updated model and models evolved for each data set (a, b and c).

	Upd. model	Model for a)	Model for b)	Model for c)
p_1	$5.500\ m$	$2.625\ m$	$7.125\ m$	$2.250\ m$
p_2	$1.20\ s$	$1.35\ s$	$1.50\ s$	$0.65\ s$
p_3	$60.5\ m$	$231\ m$	$441.75\ m$	$69.75\ m$
p_4	$181.5\ \frac{km}{h}$	$84.00\ \frac{km}{h}$	$153.9\ \frac{km}{h}$	$87.23\ \frac{km}{h}$
p_5	0.3000	0.2902	0.1012	0.9098
p_6	$181.5\ \frac{km}{h}$	$28.00\ \frac{km}{h}$	$51.3\ \frac{km}{h}$	$74.77\ \frac{km}{h}$
p_7	1.0000	0.8471	0.9294	0.6392
p_8	n/a	0.2863	0.0431	0.7294
p_9	12	2	8	11
p_{10}	12	3	5	9
p_m	n/a	0.00293	0.02248	0.00879
p_c	n/a	0.66667	0.40000	0.20000
$E_p(a)$	31.81%	**3.24%**	29.01%	24.78%
$E_p(b)$	12.69%	13.96%	**2.78%**	14.8%
$E_p(c)$	25.82%	22.98%	17.80%	**4.02%**

the Czech Republic. There is a speed limit of 130 km/h and compared to previous data set (a), vehicles are less constrained by the roadway geometry and/or friction, but they are more constrained by regulatory conditions (e.g. speed limit). Field data tend to demonstrate a fairly linear increase in speed as a function of the distance headway. The traffic is not homogenous, but it is important to note, that there is also a vehicle classification system installed here, so it was possible to classify various types of vehicles. The precision of classification is 88.5%.

The last data set (c) comes from a short and (compared to previous ones) small road segment in the city of Prague bordered from both sides with traffic lights. All the days, there is a heavy traffic with high probability of traffic jams. This facility is with no admission for heavy and/or long vehicles. Motorbikes do not often appear here. The maximum speed on this segment is restricted to 80 km/h.

All three data sets (a, b and c) were obtained using standard surveillance technologies and measured using detection loops and detection cameras (used as a supplying secondary or correlation source of data) for every day and night of the year on each facility. Therefore it was possible to measure macroscopic variables (q, u) across a certain time interval. The third macroscopic value (k), can always be calculated from the relation of the traffic flow theory (see Eq. 1). The discrete nature of traffic requires capturing time intervals of a least half a minute if we want to achieve meaningful information. Also, when time intervals exceed the duration of five minutes, certain dynamic characteristics are lost as stated in [15]. Based on this, we decided to divide every day of the year to 96 time intervals of 15 minutes each. These intervals are then divided into the two parts. First part (5 minutes) is a measurement time interval where the field data are used. Second interval (10 minutes) is thrown away. Thus we got 35040 samples of flow versus vehicle speed relation samples during the measurement interval on each facility during a year. If there is an empty one (i.e. no vehicle occurred), a sample from a given data set is deleted. The final number of usable field data samples as well as percentage of empty samples from original 35040 samples is given in the Table II.

B. Calibrated models

All parameters of the CA based microscopic traffic simulation model ($p_1 \ldots p_{10}, p_m$ and p_c), which were evolved for all three data sets $(a), (b)$ and (c) separately, are shown decoded as real values in Tab. III. All comes from the best solution of the last generation of GA. Tab. III also shows parameters of our previously manually tuned and updated CA model as introduced in [8] and [9]. Some of those manually updated values, are generally not available (GA parameters) or have a bit different meaning in our previous model. Such an example is the low speed boundary value p_6, which is identical with maximal vehicles speed p_4. This is caused by absence of the first parameter in updated model, because slowing down was performed for all available vehicles (with probability p_5). Also all vehicles in the updated model tend to always accelerate, so $p_7 = 1.0$.

Tab. III also shows the quantified error $E_p(x)$ (see Eq. 5)

$$E_p(x) = E(x)/(3 \times number\_of\_samples(x)) \qquad (5)$$

for a single sample point and for a given data set x. We also measured this error for our manually updated model with additionam maximal speed adjustment for given datasets (in the first column). It is very important to note, that some error is not bad at all, because this error is enumerated on the regressed function (e.g. some sample point could be out of the scope of this function). It can be seen that all three new calibrated models, which were obtained using our GA, are significantly better on a particular data set in comparison to our manually updated model. Moreover, all new models are also better when compared to different data sets. The only exception is the result for data set (b) which is probably due to the original purpose of updated model (made for simulating freeways). It is also remarkable in the cell length parameter (p_1), which has the biggest value meaning the biggest distance to previous vehicle in case of a complete jam. On the other side, the smallest cell length was evolved for (c), so a single vehicle (and the corresponding gap) must be modeled with two cells representing 5.5 meters. The same holds in the model for (a), where this length is 5.25 meters. In order to check whether this value is not only a result of stochastic nature of GA, Fig. 1 shows the evolution of this parameter during 125 000 generations as an average for 100 independent runs of GA. Nevertheless, it can clearly be seen that this parameter tends to converge to one particular value in all three data sets. A similar test was performed for every one evolved parameter, but due lack of space we do not illustrate them here.

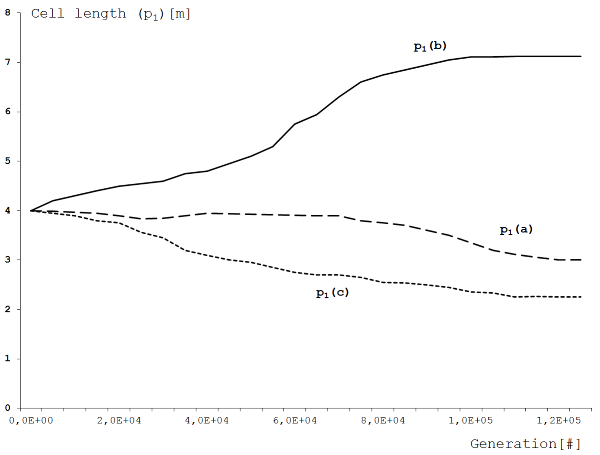

Fig. 1: Evolution of parameter p_1 in 125 000 generations for data set $(a), (b)$ and (c).

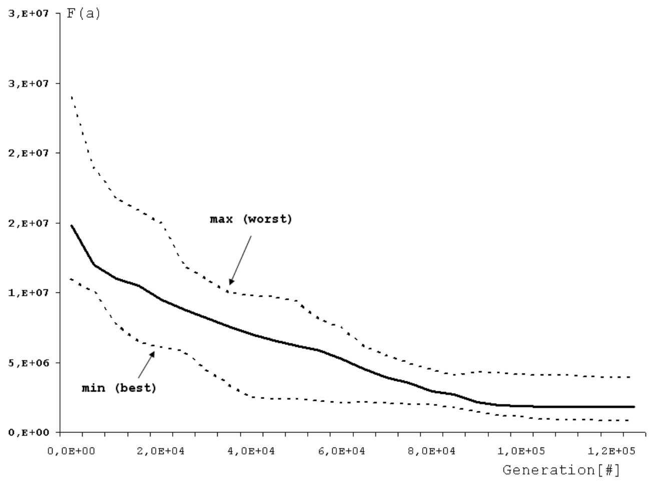

Fig. 2: Fitness $F(a)$ in all generations as an average value out of 100 independent runs with its the best and worst values when calibrating to data set (a).

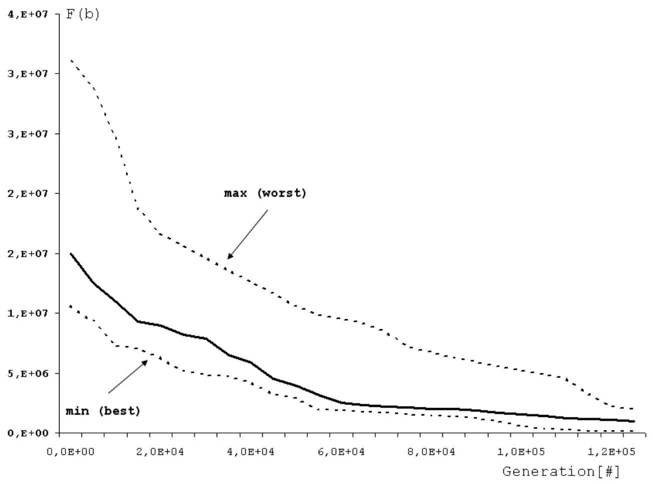

Fig. 3: Fitness $F(b)$ in all generations as an average value out of 100 independent runs with its the best and worst values when calibrating to data set (b).

The reaction time (p_2) also corresponds to what it could be expected when looking closer at the field data. The calibrated model for the second data set has again the biggest value of 1.5 seconds, that corresponds to the minimal increment of speed which is 17.1 km/h (p_1/p_2 as seen in Tab. I) and this is the biggest increment for all data sets. Surprisingly, a very big increment value could be seen also for the model calibrated to the third data set (12.46 km/h) where the data comes from often jammed short road segment, where it was thought that too big speed increments should not be supposed.

The smallest cell neighbor (p_3) was evolved for the model calibrated to (c) (i.e. 31 cells). On the other side, the biggest cell neighbor (62 cells) can be seen in model calibrated to (b). This also corresponds to nature of field data. Next parameter, the maximum allowed speed (p_4), is for all models higher than local speed restrictions as we have supposed.

For the model calibrated to (a), the probability of slowing down (p_5) is 0.2902 for vehicle speeds lower than the evolved boundary (p_6) of 28.00 km/h. The same slowing down (in case of speed lower than 51.3 km/h) occurs for 10.12% in the model calibrated to (b) and finally, up to 90.98% of vehicles are slowing down in case of their speed is lower than 74.77 km/h in the last model calibrated to (c). On the other hand, the probability of acceleration (p_7) is the highest for the second model (0.9294), then for the model calibrated to (a) (0.8471) and the lowest probability (0.6392) is in the last model. The parameter of slowing down (p_8) in case of speeds greater than the evolved boundary speed has an opposite sequence as the previous one. This could indicate that it would be possible to interoperate both of these parameters.

Parameters p_9 and p_{10} are surprisingly quite small. However, based on their convergence tests, we claim that these parameters (i.e. driver sensitivity) can be also statistically obtained for a desired road segment.

The CA traffic simulation model for the last data set was relatively easy to find which can be seen in the fastest fitness convergence. However, this model exhibits the biggest error. Models for other two sets were evolved after a longer time. It is also important to note, that completing all runs for one data set (100 runs of 125 000 generations) takes more than four days running at *Intel Xeon CPU5420 @ 2.5 GHz*. Fig. 2, Fig. 3 and Fig. 4 show the average fitness value for 100 successive runs for each data set. It can be seen, that it tends to decrease during evolution which is ensured by elitism. In these figures one can also see the best solution and the worst solution during the evolution as an average of 100 independent runs. After 125 000 generations, the quality of population is not changing dramatically. Our genetic algorithm was tuned to always find a reasonable solution after this number of generations. The whole tuning process will be described in the forthcoming paper.

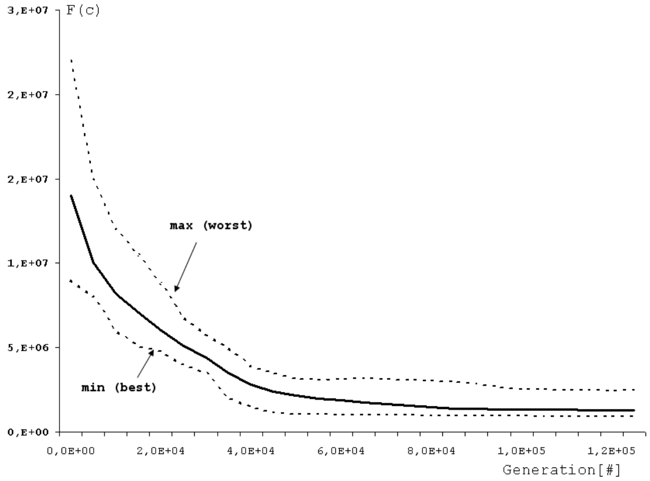

Fig. 4: Fitness $F(c)$ in all generations as an average value out of 100 independent runs with its the best and worst values when calibrating to data set (c).

VI. CONCLUSIONS

In this paper, we proposed an effective calibration method for a simple microscopic traffic simulation model. The proposed model is based on the cellular automaton, which can easily be accelerated. We utilized evolutionary approach, in particular genetic algorithm, that was able to find suitable parameters of the CA model for a given field data. For those test road segments, we increased the precision of simulator by 20.09% in average in comparison with a manually updated and tuned model. The proposed methods seem to be promising in calibration of pre-selected road segments of interest. Moreover, with this process it is possible to readjust the model to given field data which could come from standard surveillance technologies such as loop detectors in our case.

In our future work, we would like to analyze different calibrated models in greater details. For example, to compare the distribution of lead to follower distances during the time against the field data. This could be the first step to precisely predict the future traffic states or travel time. Also, it would be very interesting to derive how much data has to be used for a proper model calibration in the case when a sufficient amount of data is not available.

REFERENCES

[1] S. Maerivoet and B. De Moore, Transportation planning and traffic flow models, Technical Report No. 05-155, Katholieke Universiteit Leuven, 2005.

[2] M. Brackstone and M. McDonald, Car-following: a historical review, in Transportation Research Part F: Traffic Psychology and Behaviour, vol. 2, no. 4, Elsevier, 1999, pp. 181-196.

[3] J. L. Tripp, H. S. Morveit, A. A. Hansson, and M. Gokhale, Metropolitan road traffic simulation on FPGAs, in 13th Annual IEEE Symposium on Field-Programmable Custom Computing Machines (FCCM'05), 2005, pp.117-126.

[4] K. Nagel and D. Strippgen, Using common graphics hardware for multi-agent traffic simulation with CUDA, in 2nd International Conference on Simulation Tools and Techniques (Simutools '09), ICST 2009, Belgium, 2009, pp. 1-8, ISBN: 978-963-9799-45-5.

[5] R. Barlovic, J. Esser, K. Froese, W. Knospe, L. Neubert, M. Schreckenberg, and J. Wahle, Online traffic simulation with cellular automata, in Traffic and Mobility: SimulationEconomics Environment, 1999, pp. 117-134.

[6] A. Dupuis and B. Chopard, Cellular automata simulations of traffic: A Model for the city of Geneva, in Networks and Spatial Economics, vol. 3, no. 1, Springer Netherlands, 2003, pp. 9-21.

[7] G. H. Bham and R. F. Benekohal, A high fidelity traffic simulation model based on cellular automata and car-following concepts, in Transportation Research Part C: Emerging Technologies, vol. 12, no. 1, Elsevier, 2004, pp. 1-32.

[8] P. Korcek, L. Sekanina, and O. Fucik, A Scalable Cellular Automata Based Microscopic Traffic Simulation, in IEEE Intelligent Vehicles Symposium 2011 (IV11), Baden-Baden, DE, IEEE ITSS, 2011, pp. 13-18, ISBN 978-1-4577-0889-3.

[9] P. Korcek, L. Sekanina, and O. Fucik, Cellular automata based traffic simulation accelerated on GPU, in 17th International Conference on Soft Computing (MENDEL2011), Brno, CZ, UAI FSI VUT, 2011, pp. 395-402, ISBN 978-80-214-4302-0

[10] B. R. Hellinga, Requirement for the Calibration of Traffic Simulation Models. Department of Civil Engineering, University of Waterloo.

[11] R. Dowling, et. al., Guidelines for Calibration of Microsimulation Models: Framework and Applications, in Transportation Research Record: Journal of the Transportation Research Board, Transportation Research Board of the National Academies, vol. 1876, 2004, pp. 1-9, ISSN: 0361-1981.

[12] V. Punzo and F. Simonelli, Analysis and Comparison of Microscopic Traffic Flow Models with Real Traffic Microscopic Data, in Transportation Research Record: Journal of the Transportation Research Board, Transportation Research Board of the National Academies, vol. 1934, 2005, pp. 53-63, ISSN: 0361-1981.

[13] M. Van Aerde, H. Rakha, Multivariate Calibration of Single Regime Speed-Flow-Density Relationships, in Vehicle Navigation and Information Systems (VNIS) conference, Seattle, 1995.

[14] D. Gazis, R. Herman and R. Rothery, Nonlinear follow-the-lead models of traffic flow. Operations Research, 1961. pp. 545-567.

[15] L. H. Immers and S. Logghe, Traffic Flow Theory, Katholieke Universiteit Lueven - Faculty of Engineering, Department of Civil Engineering, Section Traffic and Infrastructure, Course H111, en. version, 2002.

[16] H. Rakha and Y. Gao, Calibration of steady-state car-following models using macroscopic loop detector data, Final Report VT-2008-01, Virginia Tech Transportation Institute, 2010.

[17] H. Rakha and M. Arafeh, Tool for calibrating steady-state traffic stream and car-following models. in Transportation Research Board Annual Meeting, Washington, D.C, 2007.

[18] S. H. Demarchi, A new formulation for Van Aerde's speed-flow-density relationship, in XVI Congresso De Pequisa e Ensino em Transportes, 2002, Natal, Brazil.

[19] K. Nagel and M. Schreckenberg, A cellular automaton model for freeway traffic, in Journal de Physique I, vol. 2, Issue 12, 1992, pp.2221-2229.

[20] K. Nagel, High-speed microsimulations of traffic flow, Ph.D. Thesis, University of Cologne, 1995

[21] P. Chakroborty and A. K. Maurya, Microscopic analysis of cellular automata based traffic flow models and an improved model, in Transport Reviews, vol. 28, issue 6, 2008, pp. 717-734.

[22] D. Chowdhury, L. Santen and A. Schadschneider, Statistical physics of vehicular traffic and some related systems, in Physics Reports 329, 2000, pp. 199-329.

[23] G. H. Bham and R. F. Benekohal, A high fidelity traffic simulation model based on cellular automata and car-following concepts, in Transportation Research Part C: Emerging Technologies, vol. 12, no. 1, Elsevier, 2004, pp. 1-32.

[24] M. F. Aycin and R. F. Benekohal, Comparison of car-following models for simulation, Transportation Research Record, vol. 1678, Washington, 1999, pp. 116-127.

[25] D. E. Wolf, Cellular automata for traffic simulations, in Physica A, vol. 263, 1999, pp. 438-451.

[26] D. E. Goldberg, Genetic Algorithms in Search, Optimization and Machine Learning, 1st Edition, Addison-Wesley, 1989, ISBN: 0201157675.